

University of Würzburg
Institute of Computer Science
Research Report Series

**Analysis of the Dynamics of CDMA
Reverse Link Power Control**

Kenji Leibnitz*, Phuoc Tran-Gia*, and John E. Miller**

Report No. 193

February 1998

**Institute of Computer Science
University of Würzburg
Am Hubland, 97074 Würzburg, Germany
Tel: (+49) 931 888-5515
Fax: (+49) 931 888-4601
leibnitz@informatik.uni-wuerzburg.de
trangia@informatik.uni-wuerzburg.de*

**** NORTEL Wireless Networks
2201 Lakeside Blvd.
Richardson, TX 75082-4399, USA
millerj@nortel.com*

Analysis of the Dynamics of CDMA Reverse Link Power Control

Kenji Leibnitz, Phuoc Tran-Gia, and John E. Miller

Abstract

In this paper we develop an analytical expression for the mobile station transmit power based on a discrete time and state space. In our model we focus on the time-varying distortions found in a CDMA reverse link channel, network delays, and the fluctuations in multi-access interference. Based on this description we are able to characterize the dynamic behavior of the power control loop and its reaction time to batch arrivals and departures. We also give an expression for exceeding the dynamic range of the discrete-step power control algorithm, allowing a systems engineer to calculate the trade-offs between capacity and coverage of the system.

1 Introduction

Code division multiple access (CDMA) is the upcoming standard RF access technology for third generation mobile communication systems. Its greatest advantage over conventional systems lies in the increase in capacity due to the application of spread spectrum technology. By spreading the transmitted signal over a larger bandwidth, the harmful effects of interference from other users can be mitigated. This robustness towards interference must be compensated at the cost of keeping the received signal strength from each mobile station (MS) at the base transceiver station (BTS) at equal levels. This, however, requires that the CDMA system overcomes the so-called “near-far” problem, where signals from users that are close to the BTS are much stronger and therefore eliminate the signals of other users located at greater distances.

To solve this problem, transmit *power control* in the reverse link (mobile-to-base path) of mobile systems based on direct sequence spread spectrum for code-division multiple-access (DS-CDMA) is performed. The air interface standard IS-95A (TIA/EIA/IS-95 1995) carefully specifies a reverse link power control algorithm and its accompanying parameters. The performance of this *signal-to-interference-ratio* (SIR) balancing algorithm based on local SIR estimates has been studied by many authors. Viterbi et al. (1993) constructed an analytical model containing inner loop processing (based on SIR) and outer loop processing based on frame error performance. Ariyavisitakul and Chang (1993) conducted a simulation study of single and multi-cell systems and examined the dependence of signal and interference statistics on step size and processing delays. D’Avella et al. (TBD) and Pincha et al. (TBD) examined the effects of power control non-idealities on performance. Distributed algorithms which use network-wide information have also been examined, see (Kim et al. 1997) and (Mitra and Morrison 1997).

The goal of this work is to formulate a comprehensive analytical model for the power control loop of Ariyavisitakul and Chang (1993). The motivation behind this goal is to find a robust model of reverse link power control which will clearly illustrate the trade-offs between system parameters and their impact on performance. System parameters include step-size, processing delay, traffic loading, loop dynamic range, and path loss. The model we propose is a Markov state space representation of the portion of the mobile transmit power controlled by the inner power control loop. This model follows naturally from the IS-95A specification since it specifies a power control step size as well as an inner loop dynamic range. These conditions result in a quantization of the reverse-link inner loop transmit power “states” that the mobile may occupy. This approach allows direct computation of the statistics of the portion of the mobile transmit power controlled by the inner loop and it results in a convenient computational model which clearly shows the effect of the system parameters on the inner loop processing. The model may be used to compute the time-dependent loop response, or to compute the probability of exceeding the mobile’s inner loop dynamic range (defined here as an outage condition) which can have serious implications on outage, coverage and capacity.

The remainder of this paper is organized as follows. Section 2 gives an overview of the power control model and the basic relations involved in the loop. In Section 3 we derive our analytical Markov chain model and its implications on the dynamics of the system. The results of these effects are given in Section 4 and it is followed by the conclusion and outlook on future work in Section 5.

2 Power Control Modeling and Basic Relations

This section describes the basic relations involved in the inner loop reverse link power control algorithm. In the following, we will be considering the model of the loop presented in (Ariyavisitakul and Chang 1993), see Fig. 1.

The main goal of the power control algorithm is to overcome the “near-far” problem, i.e., to keep the received power of all mobiles at the base station (nearly) equal and to track time-varying channel loss. This is achieved by the close interworking of two power control loops, the inner and outer loop. The outer loop evaluates the current frame error rate and adjusts the target SIR threshold accordingly. In the inner loop, the base station compares the received signal level of each mobile with the outer loop threshold in order to track the desired signal-to-interference ratio. If the mobile power is too low, the base station will transmit a “power up” command bit (“0”) on the power control subchannel of the forward link. Consequently, a too high power level will result in the transmission

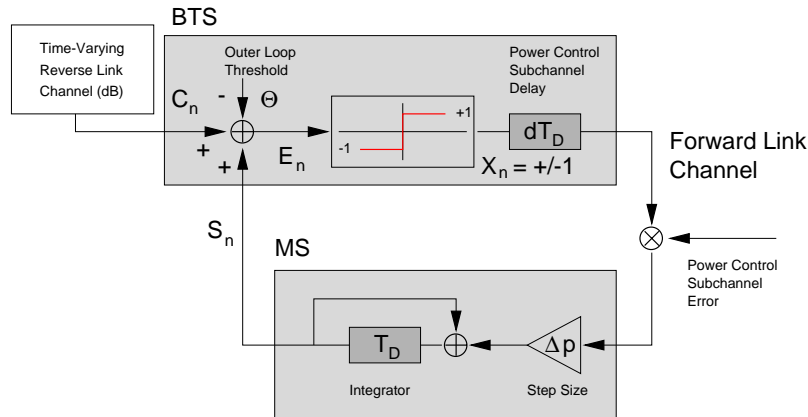


Figure 1: Model for the inner loop

of a “power down” (“1”). It is not possible for the mobile to maintain its current signal level.

The command bit is sent without error-coding, thus resulting in a higher error probability than for the other data transmitted on the forward link. It has been shown, however, that under certain conditions, power control but errors can have little impact on performance (Viterbi 1995), (Ariyavisitakul and Chang 1993).

Upon reception of the power control bit the mobile will update its transmit power by a fixed step size, predefined here to 1 dB. This update is performed every power control cycle (defined here as a time interval of 1.25 ms). The processing of the power control command requires a subchannel delay of 3 cycles causing that a power control update computed at time n will take effect at cycle $n + 3$.

3 Analytical Model of the Power Control Loop

In our analytical model we will focus on the time dynamics of the mobile transmit power. Since both, the time increments and the power updates are discrete values of 1.25 ms and 1 dB, respectively, we can model the transmit power in a discrete time and state space. In the IS-95 system the range for the MS transmit power is between -50 dBmW and 23 dBmW. In the following, we will use an abstract indexing of power levels, i.e., $j = 0, \dots, J$ with J total power levels. This generalized notation will facilitate any further work considering different power update step sizes.

Let S_n be a random variable representing the mobile transmit power at power control cycle n . We will then refer to the probability that the mobile is transmitting during n

at power level j as $s_n(j)$.

The transmission over the reverse link channel attenuates the signal that the mobile originally sent by the *channel loss*. This loss is modelled here by the random variable C_n . The base station compares the received signal with the outer loop threshold θ and determines the power control command. We model this command as the random variable X_n and define the probability for stepping up from level j as $u_n(j)$. Consequently, the probability for a “power down” command is given by $d_n(j) = 1 - u_n(j)$. Please, note that the index n indicates the time of computation of the power control command prior to the subchannel delay.

3.1 Model Parameters

As mentioned in Section 2 the aim of the reverse link power control is to provide compensation for time-varying channel losses and eliminate near-far induced multiaccess interference. This may be modelled by a control loop which forces the effective symbol energy to noise spectral density ratio $(E_S/N_0)_{\text{eff}}$ to some threshold. This section presents a system-level model for the $(E_S/N_0)_{\text{eff}}$ which includes such parameters as the subscriber population and the maximum number of active users allowed in the system. While some researchers have found that normal fluctuations in subscriber traffic have little effect on power control performance (Ariyavisitakul and Chang 1993), we wish to include it here so that we may account for the effects of batch arrivals and departures.

We may define a quantity which we will refer to as the *loading factor*:

$$F = \frac{I}{I + N} \quad (1)$$

where I is the total interference power and N is the noise power. Similar quantities have been defined by other authors (Padovani, Butler, and Boesel 1994). It is easy to show that the signal-to-interference-and-noise-ratio (SINR) is related to F by the expression:

$$\text{SINR} = \frac{\tilde{S}}{I + N} = \frac{\tilde{S}}{N} \cdot (1 - F) \quad (2)$$

where \tilde{S} is the signal power. If the system supports only a single user, the loading is zero and the $\text{SINR} = \text{SNR}$, if the loading is maximum $I \gg N$, the loading is unity and the SINR is zero.

We may derive a more direct relationship between the number of active users and the average interference. Consider that the interference power is some fraction of the interference and noise power:

$$I = \varepsilon P = \varepsilon(I + N) = (k - 1)\tilde{S} = \varepsilon(k_p - 1)\tilde{S} \quad (3)$$

where $0 \leq \varepsilon \leq 1$, \tilde{S} is the power of each interfering signal (they are all assumed to be equal), k is the number of active users and k_p is defined as the maximum number of active users supported by an interference-limited system. The *pole capacity* is approximately $k_p \approx (W/R)/(E_S/N_0)_{\text{eff}} + 1$ where W is the spreading bandwidth and R is the data bandwidth. Using these relationships we can see that $F = \varepsilon = (k - 1)/(k_p - 1)$. If we consider that $E_S \approx \tilde{S}/R$ and $I_0 + N_0 \approx I/W + N/W$, a convenient relationship for $(E_S/N_0)_{\text{eff}}$ results:

$$\left(\frac{E_S}{N_0}\right)_{\text{eff}} = \frac{E_S}{I_0 + N_0} = \frac{W}{R} \frac{\tilde{S}}{N} \cdot \left(\frac{k_p - k}{k_p - 1}\right) \quad (4)$$

So, fluctuations in the subscriber population result in a linear fluctuation in the $(E_S/N_0)_{\text{eff}}$. The quantity in parentheses represents an interference-induced loss. If k_p is large, then the arrival or departure of a few users will be negligible. However, if a batch arrival or departure occurs the fluctuation in $(E_S/N_0)_{\text{eff}}$ could be substantial. The effect of these traffic-induced fluctuations on control-loop dynamics is of particular interest here.

3.2 Gaussian Channel Model

A mobile transmits a signal to the base station at power level S_n . While traversing the reverse link channel it is being attenuated due to propagation loss, multipath effects, and shadow fading. We can therefore define the received signal at the base station $\tilde{S} = S + (\text{PL} + Z)$ as sum of the transmitted signal and the channel loss, which contains the propagation loss PL and the loss due to shadow fading Z . For our model we will use the well known Hata model (Rappaport 1996) for computing PL and shadowing will be described by a zero mean Gaussian random variable.

We can then rewrite Eqn. (4) for a given user at power control cycle n as:

$$\left(\frac{E_S}{N_0}\right)_{\text{eff}} = \frac{W}{R} + (S_n + \text{PL}_n + Z_n) - N + \frac{k_p - k}{k_p - 1} \quad (5)$$

All quantities given here are in dB.

As a first step we will include all factors except for S_n in our loop driving variable of the channel loss C_n which we will model as i.i.d. Gaussian random variable with mean $\mu_C = \frac{W}{R} + E[\text{PL}_n] + E[Z_n] - N + \frac{k_p - k}{k_p - 1}$ and standard deviation σ_C . Since we assume the thermal noise power N and the number of users k to be constant, we can leave out the time index. For the other random variables, we need to observe the mean value, indicated by $E[\cdot]$.

The probability for a “power up” command at cycle n can then be computed by comparing the $(E_s/N_0)_{\text{eff}}$ value with the threshold θ obtained by the outer loop. For the sake of simplicity we will assume here a fixed value of $\theta = 14$ dB.

$$P(\text{“power up”}) = P\left(\left(\frac{E_s}{N_0}\right)_n \leq \theta\right) = P(S_n + C_n \leq \theta) \quad (6)$$

This leads us to the probability for “power up” from a power level j as:

$$u_n(j) = P(C_n \leq \theta - j) = \frac{1}{2} + \frac{1}{2} \cdot \text{erf}\left(\frac{\theta - j - \mu_C}{\sqrt{2} \cdot \sigma_C}\right) \quad (7)$$

Since we currently have not included any time-dependent behavior of the channel, we can also drop the time index n and simply write $u(j)$. The probabilities $u(j)$ for a “power up” command depending on the mobile transmit power j are depicted in Fig. 2. Increasing the number of users in the cell results in a worse $(E_S/N_0)_{\text{eff}}$ ratio (via the multiaccess interference term) and therefore the probability of “power up” for power levels below the desired threshold increases as well.

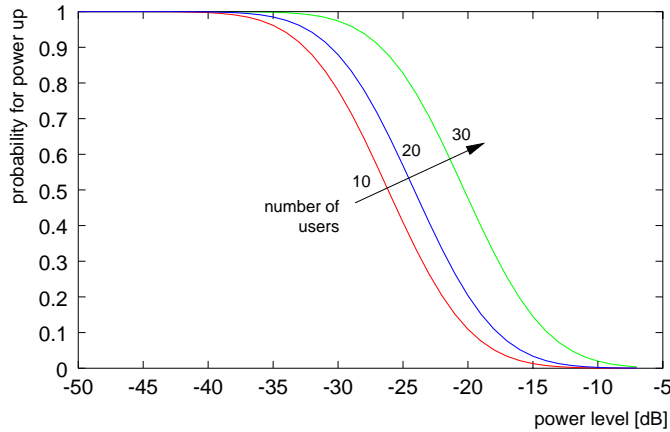


Figure 2: Probabilities for “power up” command

3.2.1 Dependency Structure and Markov Chain Description

The time dependent behavior of the inner loop can be greatly influenced by the power control subchannel delay which causes the power control command to take effect 3 time increments after the up/down command was issued. The three step delay results from a $d = 2$ step delay in Fig. 1 and an additional delay of one time increment due to mobile processing delays.

Transitions from one discrete power level to the next take place each cycle and are only performed between adjacent levels. The dependency structure of the power levels for reaching a given level j is illustrated in Fig. 3(a).

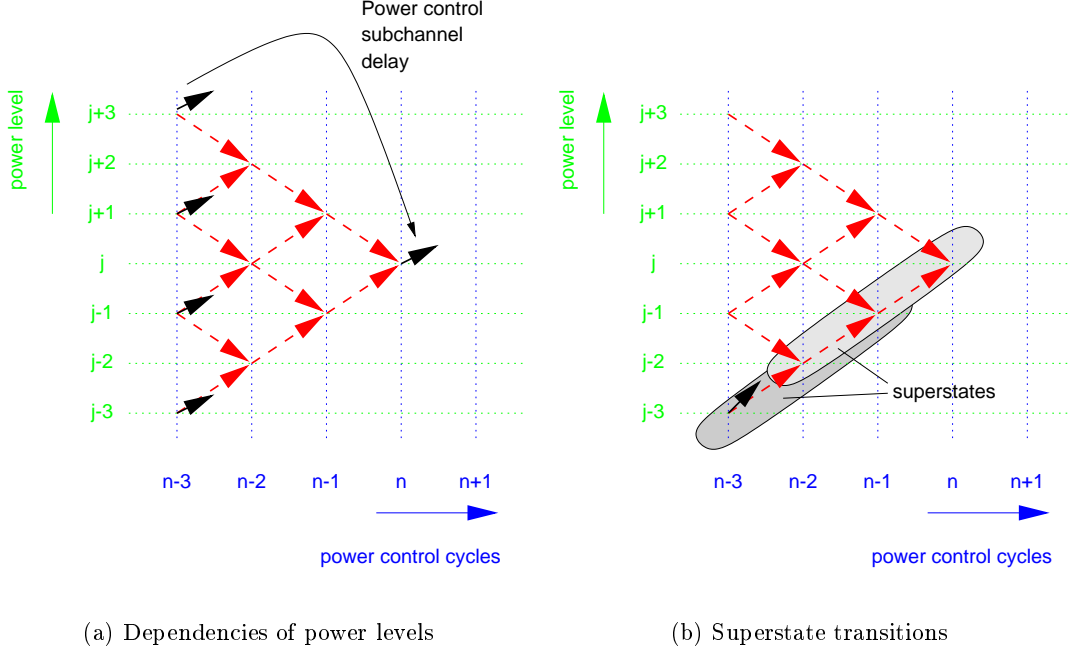


Figure 3: Power control model state transition dependencies

Fig. 3(a) illustrates that the power control command “up” for level j at time n depends on the probabilities for “power up” of the 4 possible states that could have been assumed 3 cycles before, i.e., levels $j + 3$, $j + 1$, $j - 1$, and $j - 3$ at time $n - 3$. Note that for state j it is not possible to have been in the same state 3 cycles before.

Since the probability for each state at time $n - 3$ is computed by an equivalent subtree structure, we are also dependent on the probability of reaching these originating states at time $n - 3$. We therefore cannot simply assume the probabilities $u_n(i)$ are the transition probabilities in our case because we must also include the paths for reaching these states. In order to incorporate these paths as well, we define new superstates $\bar{s}_n(j_1, j_2, j_3)$ containing 3 successive ordinary states which indicate the sequence that was taken.

$$\bar{s}_n(j_1, j_2, j_3) = P(S_n = j_3 | S_{n-1} = j_2, S_{n-2} = j_1) \quad j_1, j_2, j_3 = 0, \dots, J \quad (8)$$

Since we only have transitions between neighboring states to $j_2 = j_1 \pm 1$ and $j_3 = j_2 \pm 1$,

we can further limit the state space. In this case we have $4(J + 1)$ possible preceding superstates $\bar{s}_{n-1}(j_1, j_2, j_3)$ and a transition to superstate $\bar{s}_n(j_2, j_3, j_4)$ takes place with $u_{n-3}(j_1)$ or $d_{n-3}(j_1)$ depending on whether $j_4 = j_3 + 1$ or $j_4 = j_3 - 1$. The transitions between superstates will then look like in Fig. 3(b).

Based on these superstate transitions, it is possible to give a state space diagram at time n with the transition probabilities given by $u_n(i)$ and $d_n(i)$, see Fig. 4. The

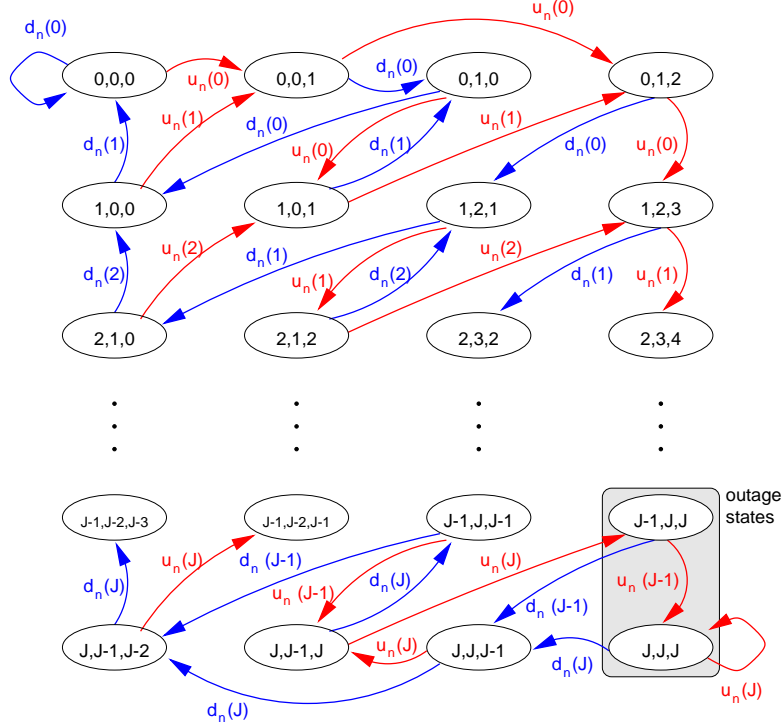


Figure 4: Superstate space of Markov chain

transition probabilities at time n can be ordered in a Matrix \mathcal{P}_n .

3.3 Non-Stationary Case

We first consider a non-stationary case, where we start off with an initial mobile transmit power distribution S_0 at time 0 and iteratively compute the successive power distribution S_n of the considered user in cycle n .

Computation of the power S_{n+1} is done in accordance to the scheme described in the previous section with consideration of the possible transition paths. The new state probabilities S_{n+1} can be computed from S_n by determining the corresponding superstate

vector \bar{S}_n and performing the power method with \bar{S}_n :

$$\bar{S}_{n+1} = \bar{S}_n \cdot \mathcal{P}_n \quad (9)$$

The transformation from \bar{S}_{n+1} to S_{n+1} yields the new state probabilities. This can be achieved easily by adding all superstates which have a common last state.

$$s_n(j) = \sum_{j_1, j_2} \bar{s}_n(j_1, j_2, j) \quad j = 0, \dots, J \quad (10)$$

Since we are interested in the dynamic behavior of the system, we will examine the reaction time until the system converges from one stable condition to another. We will focus in this paper on the impact of the power control algorithm on two important parameters: the number of users currently served within this cell and the distance of the observed user from the base station. The effects of varying these two parameters on the mean mobile transmit power will be studied. It will also be possible to work with higher moments as we obtain the complete power distribution, should this become necessary.

The choice of the initial vector at time $n = 0$ has a great impact on the speed of convergence in the system. To make sure that the system originates from a steady state and is no longer transient, we need to perform a stationary analysis, in which we will derive a power distribution that is independent of the time n . This is an estimation for a steady state distribution that we will also use in our experiments as initial power for the non-stationary experiments.

3.4 Stationary Case

In this section we assume a stationary power control case. Stationary in this sense means that the probability distributions of the random variables S_n are independent of n . We can then drop the index n denoting the time dependent power control cycle as shown in Eqn. (11) and (12). Please, note that with \bar{S} we denote the superstates in our system and not our original states representing the power levels.

$$\bar{S} = \lim_{n \rightarrow \infty} \bar{S}_n \quad (11)$$

$$X = \lim_{n \rightarrow \infty} X_n \quad (12)$$

Solution of this Markov process is straightforward (Kleinrock 1975). Since the transition probabilities of these states are given, we can obtain the solution of the state probabilities by solving the following homogeneous linear Eqn. (13).

$$\left(\bar{s}(0, 0, 0), \dots, \bar{s}(J, J, J) \right) \cdot (\mathcal{P} - \mathcal{I}) = \mathcal{O} \quad (13)$$

Here, \mathcal{I} is the identity matrix and \mathcal{P} the transition probability matrix with entries $u(j)$ and $d(j)$.

The resulting distribution of the stationary transmit power of a mobile located at a distance of 2000 m from the base station in a cell with 15 users is depicted in Fig. 5. As expected the mobile power follows a normal distribution in dB which corresponds to log-normal when transformed into linear space.

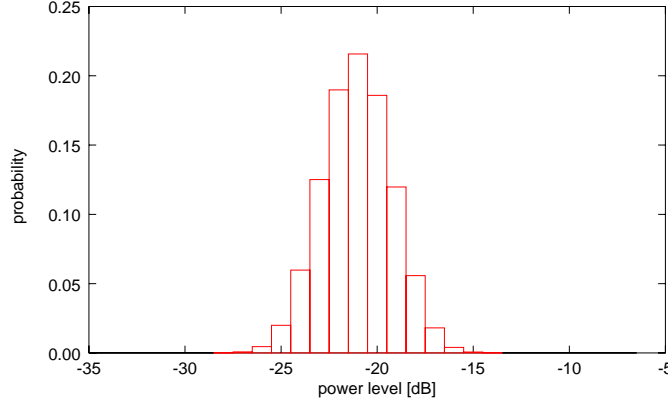


Figure 5: Stationary transmit power distribution

Figure 6(a) illustrates that the mean stationary mobile transmit power for an observed user increases with the number of users in the cell. The mean approaches the maximum power level and causes outage conditions for an increasing distance from the mobile to the base station, cf. Fig. 6(b).

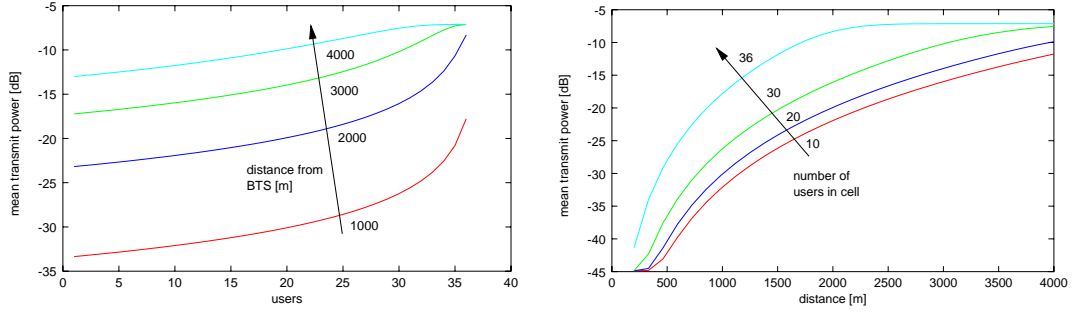
3.5 Outage probability

From our state space description it is easy to obtain an expression for the probability of *signal outage* events occurring. This is defined here as the probability that channel and/or interference conditions will require the mobile's transmitter to exceed the maximum permissible power. This occurs in the superstates $(J - 1, J, J)$ and (J, J, J) as illustrated in Figure 4.

The probability to be in an outage state can then be given as:

$$P_{\text{out}} = \bar{s}(J - 1, J, J) + \bar{s}(J, J, J). \quad (14)$$

The probability of outage as function of the number of users in the system is plotted in Fig. 7(a). Figure 7(b) shows the corresponding curve for outage as function of the distance of the observed user from the BTS.



(a) Mean power as function of users and coverage as parameter

(b) Mean power as function of distance and capacity as parameter

Figure 6: Stationary mean transmit power

Let us now define the random variable Y as the number of successive outage cases. We can easily obtain the distribution of Y under the condition that we have an outage as:

$$P(Y = i | \text{outage}) = \begin{cases} d_{J-1} & i = 1 \\ u_{J-1} \cdot u_J^{i-1} \cdot d_J & i > 1 \end{cases} \quad (15)$$

In order to get an unconditioned probability for the number of successive outage cases, we need to uncondition Eqn. (15) with P_{out} .

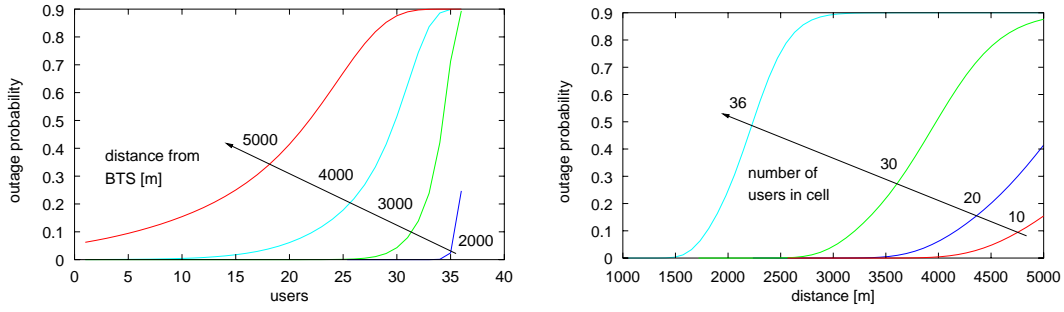
$$P(Y = i) = P(Y = i | \text{outage}) \cdot P_{\text{out}}. \quad (16)$$

The probability distribution of Y is illustrated in Fig. 8. In this scenario we assumed the user to be located at a distance of 3000 m from the BTS and varied the number of users in the cell.

Outage probability determines the *quality of service* (QoS) in a cell and is therefore an important component in network dimensioning and planning (Tran-Gia et al. 1998).

4 Results

To observe the time dependent dynamic behavior of our model we conducted several experiments where we varied the number of users in the system. We assumed an already “perfectly” power controlled system obtained by the stationary analysis with initially $k_0 = 15$ users and added $\Delta k = 5$ users to the system. We measured the power control



(a) Outage probability as function of users (b) Outage probability as function of distance

Figure 7: Stationary outage probability for varying parameters

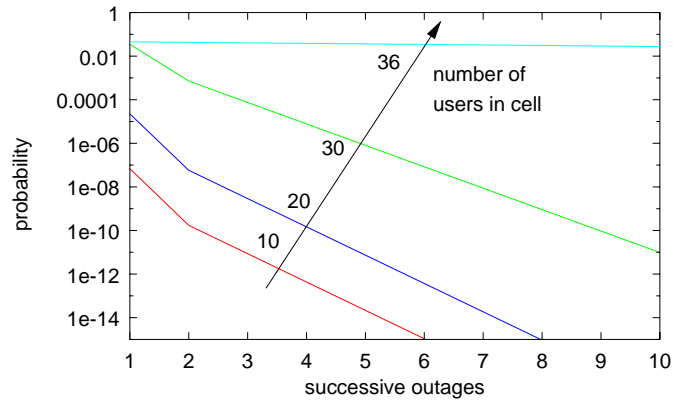


Figure 8: Probability distribution of successive outages

cycles it took for the system to again reach a stable state and compared the iterative result with the one obtained theoretically from the stationary analysis. Once stability was reached, we removed the Δk users again until we had our initial number of k_0 users. In Fig. 9 the mean power of this experiment is given. Note that the mean power overshoots the target value and converges after oscillating about the theoretical mean.

Performing the same experiment for different values of k_0 at a fixed observer distance of 1000 meters, we get Fig. 10(a) for the number of power control cycles until stability is reached when adding users and Fig. 10(b) for leaving users. Both figures show the sensitivity of the system for bulk arrivals and departures. The staircase shape of the curves stems from the fact that we do not have any fractional power control cycles as this is our smallest unit of time.

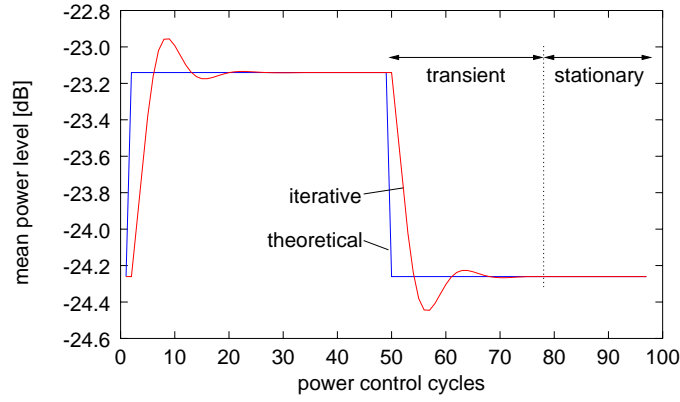
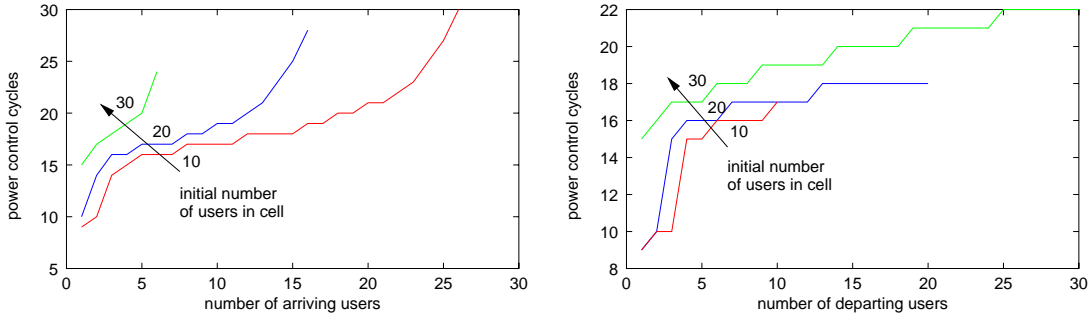


Figure 9: Mean power of non-stationary analysis



(a) Convergence time for bulk arrivals

(b) Convergence time for bulk departures

In Fig. 10(a) we add to a system already containing $k_0 = 10, 20, 30$ users Δk further users until the pole capacity is reached or the outage probability of this state exceeds 10%. It is clear that a system with a higher load requires more time to converge to a stable state. The same effect can be seen when removing Δk customers from the system. Naturally only a maximum of k_0 can be removed. It can be also seen when comparing both figures that the time for removing Δk users is shorter than for adding the same number.

When observing a user that enters the system at a certain distance in a cell that is currently loaded with $k = 10, 20, 30$ users, we obtain Fig. 10. What can be seen is that the higher loaded the cell is, the longer it takes until a stable state is achieved. The most striking fact, however, is that as long as no outage case occurs, the time for convergence is independent of the distance of the new user.

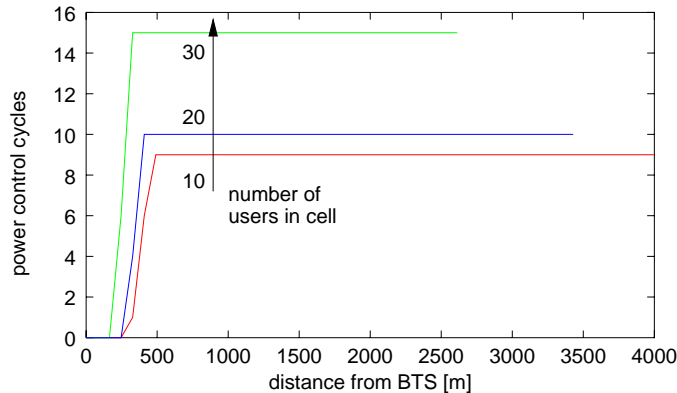


Figure 10: Convergence time over the distance from the BTS

5 Conclusion and Outlook

In this paper we presented a new analytic description of the reverse link power control in an IS-95 CDMA system. We observed that the transmit power for an arbitrary observed mobile user follows a log-normal distribution and is very sensitive to the current level of multiaccess interference in the cell. This has an effect on the quality of service in the cell in terms of increased signal outage probability. The variation of the system parameter settings showed that the reaction time for batch arrivals and departures in the cell is also mainly influenced by its current load, but less dependent on the distance-induced propagation loss.

Our approach so far only considered an *additive white Gaussian noise* (AWGN) channel with no time dependent behavior. In reality, however, correlations in the fading channel cause the propagated signal to fluctuate at a greater degree. One of our next aims is therefore to include a model that considers fading in a more realistic manner by modifying the loop driving variable.

The results presented here include the inner loop only (which uses SIR as the performance measure) and do not (yet) include outer loop processing (based on frame-error statistics) (Sampath et al. 1997). Another possible extension of the current model is to include the effects of the open-loop power control which would allow direct computation of the total mobile transmit power statistics. Both of these topics are slated as future work.

Acknowledgement

The authors would like to thank Wolfgang Jodl for his programming skills as well as Nikhil Jain and Mohamed Landolsi (NORTEL Wireless Networks, Richardson) and Notker Gerlich (University of Würzburg, Germany) for the valuable discussions and help during the course of this work. Part of this work has been supported by NORTEL External Research.

References

- Ariyavisitakul, S. and L. F. Chang (1993, November). Signal and interference statistics of a CDMA system with feedback power control. *IEEE Transactions on Communications* 41(11), 1626–1634.
- D’Avella, R., D. Marizza, and L. Moreno (TBD). Power control in CDMA systems: Performance evaluation and system design implications. *TBD*.
- Kim, D., K. Chang, and S. Kim (1997, May). Efficient distributed power control for cellular mobile systems. *IEEE Transactions on Vehicular Technology* 46(2), 313–319.
- Kleinrock, L. (1975). *Queueing Systems*, Volume 1. John Wiley & Sons.
- Mitra, D. and J. A. Morrison (1997, March). A novel distributed power control algorithm for classes of service in cellular CDMA networks. In *Proc. of the Sixth WINLAB Workshop on Third Generation Wireless Information Systems*, New Brunswick, NJ, pp. 141–157.
- Padovani, R., B. Butler, and R. Boesel (1994, June). CDMA digital cellular: Field trial results. In *Proc. 44th IEEE Veh. Tech. Conf.*, Stockholm, Sweden, pp. 11–15.
- Pincha, R., Q. Wang, and V. K. Bhargava (TBD). Non-ideal power control in DS-CDMA cellular. *TBD*.
- Rappaport, T. S. (1996). *Wireless Communications – Principles & Practice*. Upper Saddle River, NJ: Prentice Hall.
- Sampath, A., P. S. Kumar, and J. M. Holtzman (1997, May). On setting reverse link target SIR in a CDMA system. In *Proc. of the IEEE 47th Veh. Tech. Conf.*, Phoenix, AZ, pp. 929–932.
- TIA/EIA/IS-95 (1995, July). Mobile station – base station compatibility standard for dual-mode wideband spread spectrum cellular systems. Technical report, Telecommunications Industry Association.

- Tran-Gia, P., K. Leibnitz, and N. Jain (1998). Code division multiple access wireless network planning considering clustered spatial customer traffic. *submitted*.
- Viterbi, A. J. (1995). *CDMA - Principles of Spread Spectrum Communication*. Wireless Communications Series. Addison-Wesley.
- Viterbi, A. J., A. M. Viterbi, and E. Zehavi (1993, April). Performance of power-controlled wideband terrestrial digital communication. *IEEE Transactions on Communications* 41(4), 559–569.